Low-density, microcellular polystyrene foams

J. H. Aubert and R. L. Clough
Sandia National Laboratories, Albuquerque, New Mexico 87185, USA
(Received 5 February 1985)

Numerous applications have been identified for low-density, microcellular, polymeric foams. In this paper the authors describe a general technique to produce foams of this type with organic-soluble polymers, in particular polystyrene. Open-celled polystyrene foams have been developed with densities of 0.02–0.2 g cm^{-3} and uniform cell sizes of 1–20 μm. By using well-characterized polymers the authors have related form morphology to the phase diagram of the polymer/solvent system employed.

(Keywords: polystyrene; foam; microcellular; phase diagram)

INTRODUCTION

We have developed a technique to produce low-density, microcellular polystyrene foams[1]. The foams are made using a phase-separation technique and have cell sizes which are one or two orders of magnitude smaller than conventional foams of similar density. For example, polystyrene foams have been made by this process with densities of 0.02–0.20 g cm^{-3} and with cell sizes of 1–20 μm, while a polystyrene foam made conventionally by thermoplastic foam extrusion and having a similar density would have a cell size of 100–200 μm or more. In addition, the foams are isotropic and the cell size is very uniform. The foams have an open-cell structure. We report here on our results for polystyrene foams; however, our technique is general and could be applied to any polymer for which suitable solvents could be found. For example, low-density isotactic polystyrene and poly(methyl methacrylate) microcellular foams have been made with this technique.

We have identified a number of novel uses for this type of foam material. Low-density, microcellular foams have been sought for use in multishell fusion targets for laser interaction experiments[2,3]. If the foam cell size is sufficiently small, ~ 1 μm, then the foam can smooth the implosion, making it more spherically symmetric. Recently, similar foam material has been investigated for use in the development of a laboratory X-ray laser[4]. In this application a doped foam is used as the laser medium. Medical uses of microcellular foams have been identified[5] as artificial skin and blood vessels. The small cell size and high surface area also make these materials of potential interest as filters, catalytic substrates, and model porous media.

Some processes already exist to produce microcellular foams, such as classical phase inversion, sintering, and nuclear bombardment techniques, but in general these processes are restricted to higher densities, usually greater than 0.1 g cm^{-3}. A similar process to produce filled microporous polymers has been described in the patent by Castro[6]; however, his process is again restricted to higher densities (greater than 0.1 g cm^{-3}). Young *et al.*[3] have reported on a process similar to Castro's for one specific organic polymer (poly(4-methyl-1-pentene), or TPX). They were able to obtain foams with densities as low as 0.02 g cm^{-3}. Their process takes advantage of a gel which forms from the polymer solution. Similarly, Rinde[7] described a method to make low-density, microcellular foams from cellulose acetate. This method also results in the formation of a gel. Our process does not result in a gel; although it would work equally well if a gel did form. A number of authors[2,3,4] have also developed low-density, microcellular foams made from water-soluble polymers. Rand[4] has been able to produce poly(acrylic acid) form with a density as low as 0.003 g cm^{-3} for use as a laser medium.

Our polystyrene foams are unique for a number of reasons. By using narrow molecular weight distribution atactic polystyrene, we have gained control over many of the thermodynamic variables which are important in foam formation and affect both foam morphology and cell size. The many solvents available for atactic polystyrene and the range of molecular weights available have allowed us thoroughly to investigate these variables. This control enabled us to make a variety of foams meeting specifications for many different applications. We believe that we have produced the lowest density microcellular polystyrene foams to date[1]. In addition, this control has allowed us to study the physics of foam formation, which has been equally important in the development of a variety of foams. This understanding should help to guide development of other foams[2-7] and also of microporous polymer membranes[8], which can be formed by similar processes.

By the use of unidirectional cooling (during phase separation and solvent freezing) and rigorous degassing of solutions, it is possible to produce homogeneous, defect-free foam. The foams are dimensionally stable at room temperature and can be handled and even machined.

* This work was done at Sandia National Laboratories and supported by the US Department of Energy under Contract No. DE-A304-76DP00789.

0032-3861/85/122047-08$03.00

PHASE SEPARATED FOAMS

Foam morphology

The basic process is to first dissolve a polymer (e.g., polystyrene) in a suitable solvent (e.g., cyclohexane). The solution is then placed into a mould and the mould cooled rapidly until the solvent is frozen. Next, the solvent is removed by freeze-drying, leaving behind the polymer as a foam. The density of the foam is determined by the original concentration of polymer in solution. The morphology of the foam is determined either by liquid–liquid phase separation, which may occur prior to freezing of the solvent, or liquid–solid phase separation, which occurs when the solvent freezes. If liquid–liquid phase separation occurs the resulting foam is isotropic and has a small cell size (e.g., 10 μm). If only liquid–solid phase separation occurs then the resulting foam is anisotropic with a sheet-like morphology and a large separation between folds in the sheets (e.g., 100 μm). Usually an isotropic morphology is desired, but there may be some instances where directionality in the foam is advantageous. *Figure 1* schematically shows the basic process[1].

Figure 2 shows a typical temperature *versus* composition phase diagram for a polymer–solvent system. The curve A is the binodal and the curve B is the spinodal. Between these curves, solutions will undergo liquid phase separation by nucleation (either homogeneous or heterogeneous nucleation). Below curve B the solution will undergo spontaneous liquid phase separation without the requirement of nucleation. Points along curves B are called spinodal temperatures and the maximum of the spinodal curve is the critical point. The theta point[9] of the solution occurs somewhat above the critical point (depending on molecular weight) and is defined as the temperature where binary thermodynamic interactions are zero (2nd virial coefficient vanishes). This is identical to the critical temperature only for polymers of infinite molecular weight. Curves C and D below the curves A and B are the freezing point curve of the solvent. A typical quench is shown by the arrowed line. The solution moves from where it is a homogeneous solution to below the curve B, at which time it spontaneously phase separates. Subsequently the quench lowers the temperature sufficiently so that the solvent freezes.

In the usual instance, where an isotropic morphology is desired, one must pick a solvent or cosolvent system in which the polymer will phase separate at a temperature

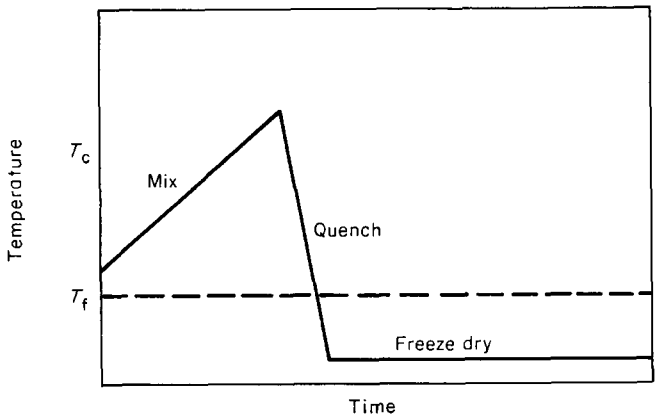

Figure 1 Basic process for making microcellular foams. T_c is the critical temperature for liquid phase separation; T_f is the freezing point of the solvent

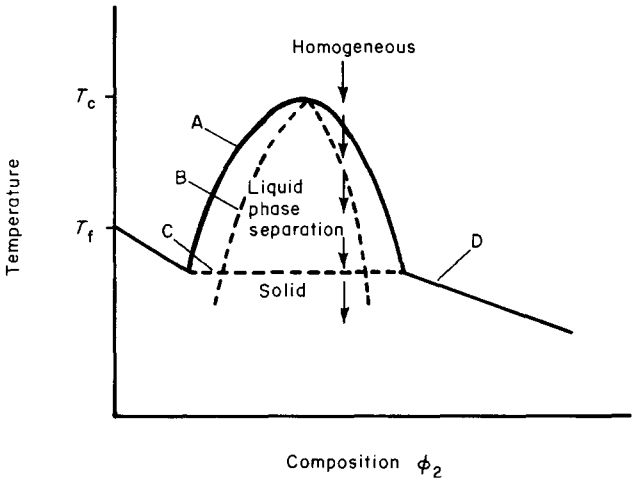

Figure 2 Typical polymer–solvent phase diagram

higher than where the solvent freezes. For some polymers a large choice of solvents exists satisfying this requirement. For many commercially important polymers, suitable solvents can be found from published lists of theta solvents for that polymer. The 'Polymer Handbook'[10] is one such reference that lists theta solvents and theta temperatures for many polymers. One example is polystyrene (PS) in cyclohexane (CH). The theta temperature is 34.6°C[10] and the freezing point of cyclohexane is 6.5°C[11]. Hence, there is a good chance that solutions will liquid phase separate prior to freezing. In fact this supposition is supported by the observation that the solutions become cloudy before freezing. A schematic of the phase diagram for PS–CH and the foam morphology obtained are shown in *Figure 3*. The foam is isotropic with a mean cell size of ~10 μm. In stark contrast to this, *Figure 4* shows a schematic of the phase diagram for PS–benzene (B) and the foam morphology obtained. In this case no theta point is listed for PS–B, and in fact no clouding of the solution is observed before freezing of the benzene. Hence, the morphology is determined by liquid–solid phase separation. As benzene crystallizes, it excludes polymer to the grain boundaries, which results in the sheet-like morphology observed in *Figure 4*. The correlation between foam morphology and the theta and melting temperatures has been confirmed for many other solvent systems that we have used in conjunction with PS. The morphologies of four of these are shown in *Figure 5*. If liquid phase separation occurs prior to solvent freezing, then the foams are isotropic with small cells (e.g., 10 μm). If no liquid phase separation occurs prior to solvent freezing, then the foams are anisotropic with a sheet-like morphology and with relatively large spacings between folds in the sheets (e.g., 100 μm).

Liquid phase separation

Two types of liquid phase separation can occur, either nucleated (binodal) or spontaneous (spinodal), as is shown in *Figure 2*. We think that spinodal decomposition is the dominant mode in the formation of our foams. This view is based on several experiments that were performed on a well-characterized system (phase diagram established). *Figure 6* shows spinodal curves that were experimentally determined[12] for cyclohexane solutions of four narrow molecular weight distribution samples of polystyrene.

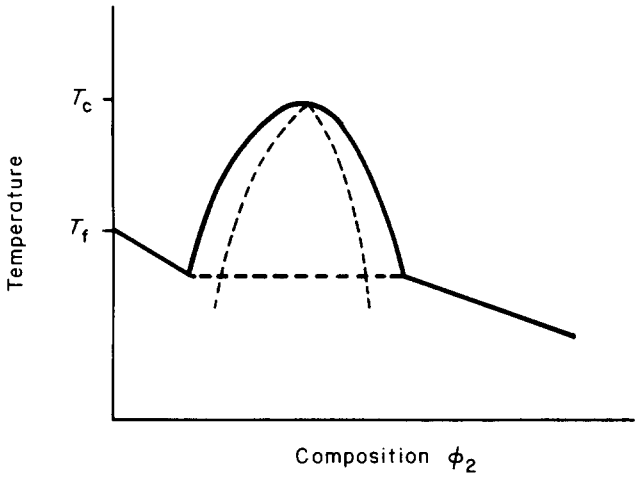

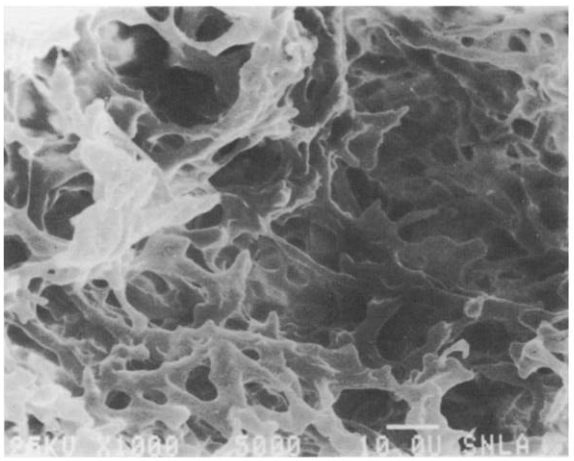

Figure 3 Schematic of the phase diagram for PS–CH ($\bar{M}_n = 1.8 \times 10^6$) and the resulting foam morphology

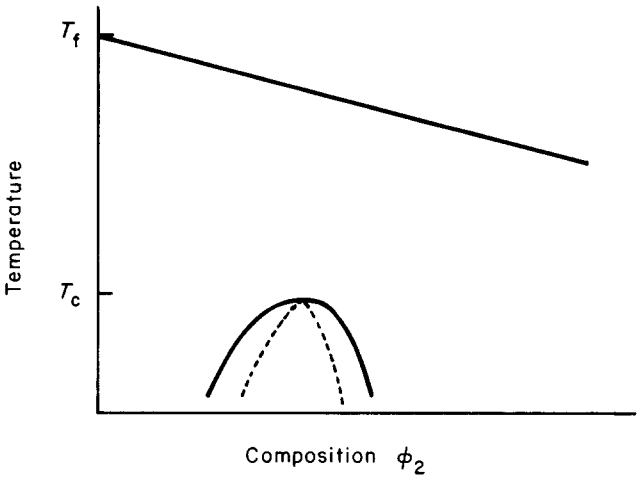

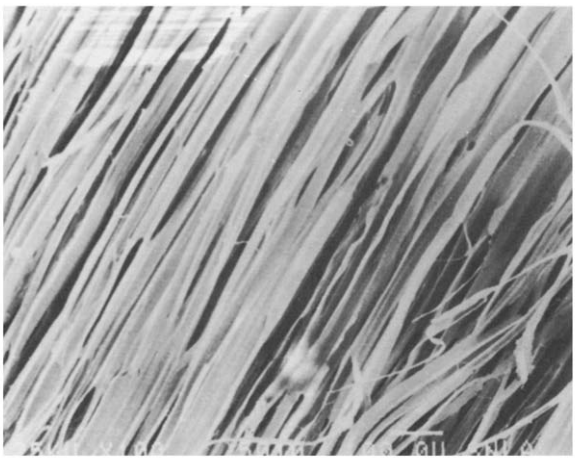

Figure 4 Schematic of the phase diagram for PS–B ($\bar{M}_n = 1.8 \times 10^6$) and the resulting foam morphology

The solid lines in *Figure 6* are predictions of the spinodals based upon the Flory–Huggins equation[9] and an empirical expression for the Flory interaction parameter χ[12]. The Flory–Huggins equation is:

$$\frac{\Delta F_m}{V_T} = RT\left[\frac{\phi_1}{\bar{V}_1}\ln\phi_1 + \frac{\phi_2}{\bar{V}_2}\ln\phi_2 + \frac{\chi\phi_1\phi_2}{\bar{V}_1}\right] \quad (1)$$

where ΔF_m is the free energy of mixing, V_T is the solution volume, R is the gas constant, T is the absolute temperature, ϕ_1 and ϕ_2 are the volume fractions of solvent and polymer respectively, $\bar{V}_1$ and $\bar{V}_2$ are the specific volume of solvent and polymer respectively, and χ is the interaction parameter. An empirical expression for χ for polystyrene in cyclohexane is[12]:

$$\chi = 0.2035 + 90.5/T_c - 2600P^{-0.38}(1/T - 1/T_c) + 0.3092\phi_2 + 0.1554\phi_2^2 \quad (2)$$

where T_c is the critical temperature and P is a molecular weight dependent parameter which for PS in CH is $M/116.4$. Using these expressions the spinodal curves, the critical temperature, and the critical volume fraction can be determined by standard techniques[13]. For a molecular weight of 1.8×10^6, the critical volume fraction, ϕ_2^c is predicted to be 0.0262.

We have successfully made foams at this critical volume fraction, and even below it, as well as above it. The foam morphology in each case was identical. At the critical point presumably only spinodal decomposition can take place since the cooling path passes directly into the spinodal region. Since foam morphology is insensitive to concentration, it is reasonable to assume that spinodal decomposition is the mechanism even away from the critical point. In addition, if nucleation were the mechanism, then below the critical volume fraction the polymer-rich phase would nucleate and the solvent-rich phase would be the continuous phase. It is unlikely that nucleated polymer phases could join into the high surface area interconnected structures that these foams exhibit. As discussed below, spinodal decomposition naturally results in interconnected bicontinuous phases, which is the structure of these foams.

Another reason that we think spinodal decomposition is the dominant liquid phase separation mechanism is the fact that our process requires very fast quench rates in order to produce foam. A typical quench rate for this to occur is 100°C min^{-1}. We have observed that for slow quench rates, which favour nucleation and growth, we produced only powder and not a foam. High quench rates will drive the solution through the binodal quickly and into the spinodal region. During the passage through the binodal, some nucleation probably occurs even for fast quenches. However, once in the spinodal region the

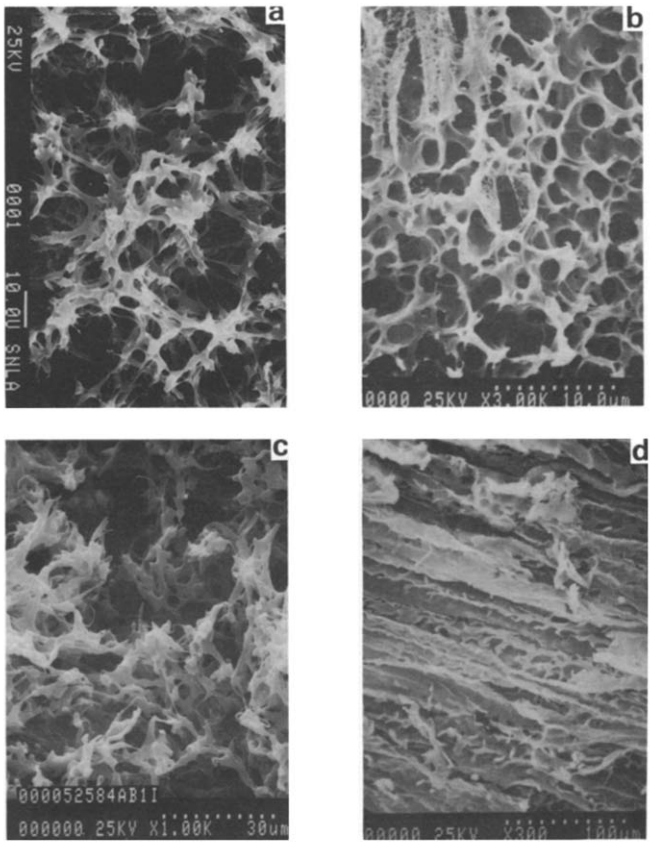

Figure 5 Liquid–liquid phase separation occurs prior to solvent freezing: a, dioxane (D): Isopropanol (I)/55:45; b, D: *n*-hexane/38:62; c, benzene (B): I/64:36. Liquid–solid phase separation occurs in d, dioxane (D)

mechanism is spinodal decomposition. Any nucleated phases will then be incorporated into the spinodal structure[14].

Rate effects

Cahn[15] has described the spinodal structure of a liquid phase separating binary liquid at low times. His result, written in terms of volume fractions, is given by:

$$(\phi_2-\phi_2^0)=\sum_{\underset{\sim}{\beta}_m}\exp[R(\underset{\sim}{\beta})t] \times[A(\underset{\sim}{\beta})\cos(\underset{\sim}{\beta}\cdot\underset{\sim}{r})+B(\underset{\sim}{\beta})\sin(\underset{\sim}{\beta}\cdot\underset{\sim}{r})] \quad (3)$$

In this equation, $\underset{\sim}{\beta}$ is a 3-dimensional wave vector, $\underset{\sim}{\beta}_m$ is the wave vector which receives maximum amplification, $R(\underset{\sim}{\beta})$ is the amplification factor, t is the time ($t=0$ corresponds to the moment in time when the solution is dropped below the spinodal curve), $\underset{\sim}{r}$ is the position in space with respect to an arbitrary origin (the solution is assumed unbounded), and ϕ_2^0 is the average polymer volume fraction. A and B are determined by the initial ($t=0$) thermal concentration fluctuations. This equation states that spinodal decomposition results in polymer volume fraction fluctuations ($\phi_2-\phi_2^0$) which grow exponentially in time (at short times) and are periodic in space. Hence, spinodal decomposition produces bicontinuous phases.

The amplification factor $R(\underset{\sim}{\beta})$ is given by:

$$R(\underset{\sim}{\beta})=-L\frac{N_{AV}}{M}w_2^2\beta^2\left[\frac{\partial^2}{\partial\phi_2^2}\left(\frac{\Delta F_m}{V_T}\right)+2\kappa\beta^2\right] \quad (4)$$

where L is the polymer mobility (obtained from experimental values of the diffusion coefficient), w_2 is the volume of a polymer molecule, and κ is an interfacial energy parameter. In Cahn's solution the only wave vector counted is the one which has maximum amplification. The maximum corresponds to wave vector and wavelength ($\lambda=2\pi/|\underset{\sim}{\beta}_m|$) given by:

$$|\underset{\sim}{\beta}_m|=\sqrt{-w_2^2\left(\partial^2\left(\frac{\Delta F_m}{V_T}\right)\Big/\partial\phi_2^2\right)\Big/4\kappa}=2\pi/\lambda \quad (5)$$

The interfacial energy parameter, κ, has been approximated by Debye[16] to be:

$$\kappa=\frac{\langle s^2\rangle}{6}\frac{kT}{w_2}\chi \quad (6)$$

where the mean-square radius of gyration of a polymer coil is $\langle s^2\rangle$. This can be approximated from intrinsic viscosity data[17]. This equation accounts for energetic effects (χ), but neglects entropic effects. In addition, the length scale used in equation (6), ($\langle s^2\rangle$), is not rigorous. Despite these approximations, equations (1), (2), (5) and (6) can be used for PS–CH to give an approximation of the wavelength expected. For PS of molecular weight 1.8×10^6, volume fraction $\phi_2=0.05$, and a quench temperature of 274.4 K, which is the undercooled point at which the solvent in this solution freezes, the wavelength prediction is 0.70 μm. This prediction also neglects the fact that the quench is not instantaneous but continuous. However, Huston *et al.*[14] have determined that instantaneous and continuous cooling lead to qualitatively the same results.

Comparison of this prediction with the SEMs in *Figures 3* and *5* shows that, usually, we see a cell size about an order of magnitude greater than the predicted value.

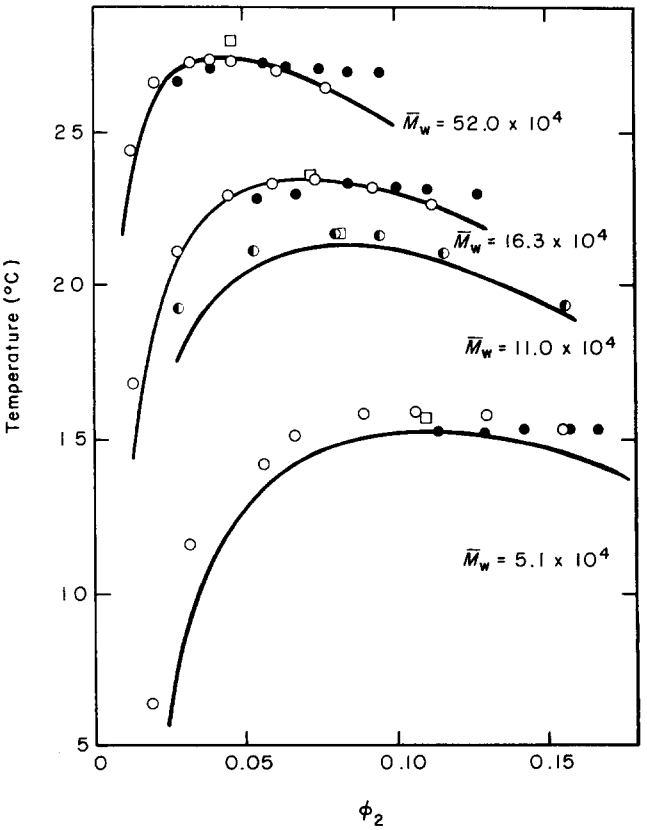

Figure 6 Spinodals for cyclohexane solutions of four narrow molecular weight distribution samples of polystyrene with the indicated M_w. (○): Scholte; (●): Derham *et al*; (◐): Kojima *et al.* (□): observed critical points, Koningsveld *et al.* From Fujita and Teramoto[12]

This implies that the foam structures typically seen are not early stage spinodal structures, but are late stage structures. A late stage (or ripened) structure is one that develops from the early stage structure by a flow or diffusion process into a coarsened structure. The driving force for this motion is the reduction of interfacial area and, hence, interfacial energy. The resistance to this motion arises from the viscosity or mobility of the polymer-rich phase. This discussion indicates that the coarsening process is a quench-rate dependent process. For example if the quench rate is sufficiently high, the early stage structure may be frozen in. On the other hand, a slower quench rate will allow the structure more time to coarsen.

An example of this effect is shown in *Figure 7*. Both micrographs are of the same foam, which was made from a high volume fraction ($\phi_2 = 0.09$) of PS in CH. The difference is in the quench rates. The *Figure 7b* shows the bottom of the foam, where the quench rate was high. Here, the structure is fine, with a cell size of less than 1 μm. *Figure 7a* shows the top of the foam, where the quench rate is much lower because of the insulation effect of the material below it. Here, it is obvious that the structure is coarsened, with a cell size of around 10 μm. Significant variation of cell size with quench rate is observed only with higher density foams, such as those shown in *Figure 7*.

Figure 7 is interesting because it demonstrates a quench rate effect and shows that a fine structure can be formed under some conditions. Usually, however, a uniform morphology is desired in a foam. This would require a high quench rate throughout the foam thickness. Besides varying the cooling rate, another way to control cell size is to use a cosolvent system, for example dioxan and isopropyl alcohol, D:I. By varying the cosolvent ratio we can move the phase diagram while keeping the freezing point of the solvents essentially the same. If we make the solvent worse for polystyrene (by using more isopropyl alcohol), then we can move the spinodal curve arbitrarily close to the freezing point of dioxan in the solution. This has qualitatively the same effect as a higher quench rate throughout the solution, because now as soon as the solution liquid phase separates, the solvent freezes. Thus, the early-stage structure is frozen in, and this occurs through the foam thickness.

An example of this is shown in *Figures 8, 9* and *10*. In each Figure we show a schematic of a pseudo two-component phase diagram appropriate for the cosolvent ratio and a picture of the foam obtained. Since three components are present, the two-component phase diagram is only a qualitative picture that shows how the spinodal temperature is lowered as the solution becomes richer in the good solvent. In *Figure 8* the cosolvent ratio is 55:45/dioxane:isopropanol. Liquid phase separation occurs well above the temperature where dioxan freezes. Hence, the foam structure obtained is coarsened, with a cell size around 10 μm. In *Figure 9* the cosolvent ratio is 60:40. Liquid phase separation occurs just before dioxan freezes. Throughout the foam the structure is extremely fine, with a cell size around 1 μm. In *Figure 10* the cosolvent ratio is 80:20. In this case liquid phase separation does not occur until most of the dioxan has frozen. The foam structure is basically sheet-like and anisotropic. The fine structure on the sheets indicates that some liquid phase separation does occur before all of the solution freezes. If the starting solution is made richer in dioxan, then the amount of fine structure on the sheets decreases.

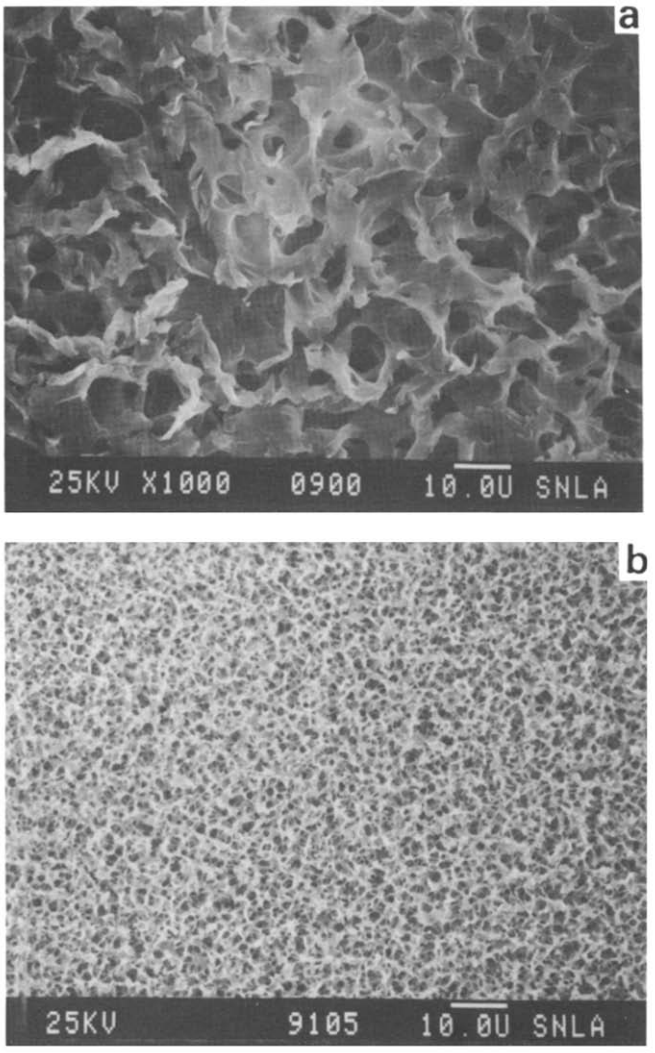

Figure 7 (a) (Coarse structure) and (b) (fine structure) of a foam made from PS ($\bar{M}_n = 1.8 \times 10^6$) in CH at a volume fraction, $\phi_2 = 0.09$

Effects of molecular weight

Polystyrene is almost unique because it is available in a wide range of molecular weights, and because even high molecular weight polystyrene can be obtained with a narrow molecular weight distribution. This degree of freedom is important to the study of phase-separated foams, but it has also been important in developing foams with a wide range of densities.

One effect of molecular weight is that it changes the phase diagram of the polymer. Hence, for a given process the spinodal temperature changes. Obviously, a different molecular weight has a different molecular size, so that the early-stage spinodal structure size is different, equation (6). Also, the early and late stages develop at a different rate, since mobility is strongly affected by molecular weight. The greatest effect of molecular weight, however, is that it is directly related to the lowest density of foam that can be made.

Spinodal decomposition results in bicontinuous phases only if the volume fraction of polymer is high enough for the polymer coils to overlap in solution. This volume fraction is called ϕ_2^* and is strongly molecular weight

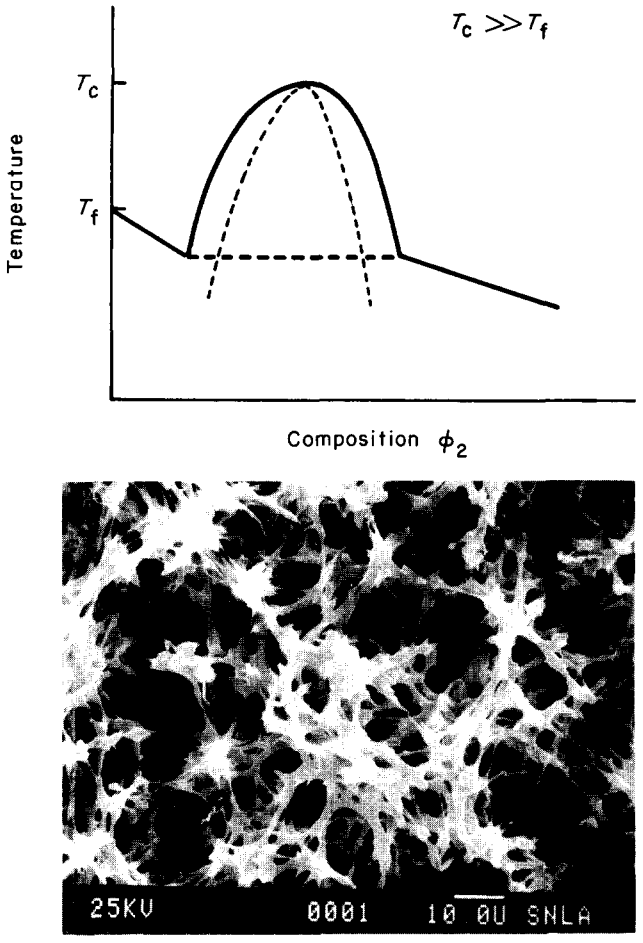

Figure 8 Pseudo two-component phase diagram and SEM of foam obtained for PS ($\bar{M}_n = 1.8 \times 10^6$, $\phi_2 = 0.03$) in 55:45 dioxan–isopropyl alcohol

dependent[18]. The volume fraction is best determined by light scattering, but is often approximated by

$$\phi_2^* = \frac{w_2 N_{AV}}{M[\eta]} \qquad (7)$$

where $[\eta]$ is the intrinsic viscosity. We have estimated ϕ_2^*, *Table 1*, for various molecular weights by equation (7) and an expression for $[\eta]$[10]. We have not been able to make foams below, or near ϕ_2^*

We have not studied in detail the effect of polymer molecular weight on the strength of resultant foams. We expect, however, that molecular weight will only affect foam strength at lower molecular weights. We have found that the use of molecular weights under about 10^5 has not been very successful in attempts to produce foams. We are currently studying crystallizable (isotactic) polystyrene and expect that this will enhance the strength of the foams. Successful foams have also been made with a broad molecular weight distribution polystyrene of weight-average molecular weight 851 000, and polydispersity ($\bar{M}_w/\bar{M}_n$) equal to 5.93.

EXPERIMENTAL

Processing

Foams were produced as follows. First, the polymer and solvent were refluxed to bring about dissolution. The dissolved air was removed from the solution during reflux under reduced pressure. The solution was then poured into a clean, warm mould. The mould was sealed, and placed under reduced pressure for about 90 s. This final degassing step was intended to remove all of the dissolved gases. From this point on, the solution in the mould was never exposed to the atmosphere again. The most important step in producing high quality foams was degassing. If any dissolved gas remained, it was evolved when the solvent froze. Any evolved gas can easily be trapped in the freezing solvent and this creates macroscopic voids in the final foam.

Since degassing can be an endothermic process and solvent evaporation (which also occurs under reduced pressure) is endothermic, the solution cooled during this step. Severe cooling can precipitate some of the polymer. To compensate for this cooling, the samples were always annealed after degassing. This was carried out by placing the sealed moulds into an oven (at 50°C for about 15 min in the case of polystyrene–cyclohexane). The annealing process was interrupted periodically so that the moulds could be shaken to facilitate dissolution.

Once annealing had taken place, the moulds were placed on a cold surface to freeze the solution. It is necessary to keep the solution stationary while freezing so that the phase-separated structure is not broken. Our cold plates consist of large copper blocks having a high

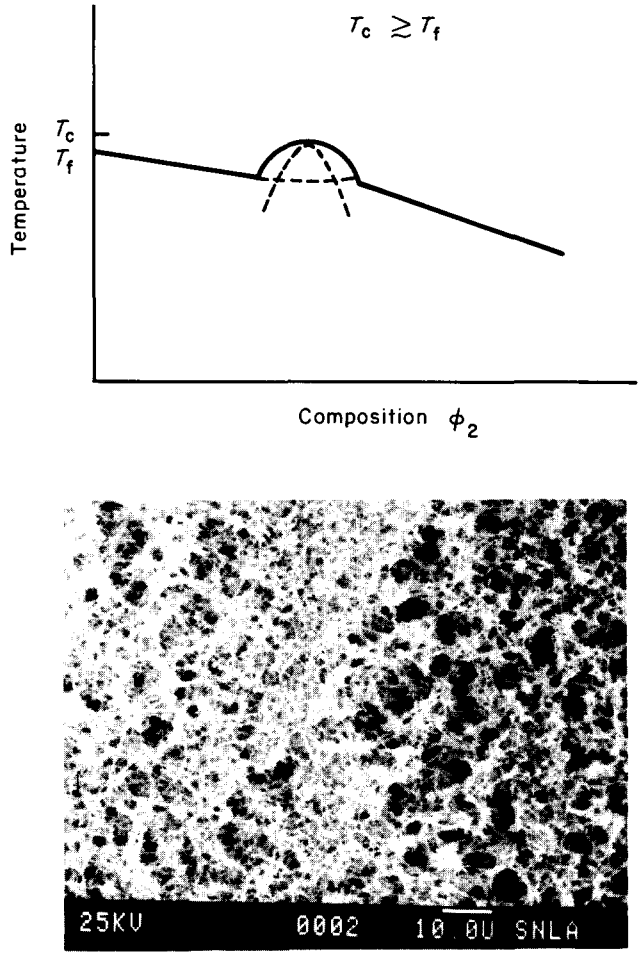

Figure 9 Pseudo two-component phase diagram and SEM of foam obtained for PS ($\bar{M}_n = 1.8 \times 10^6$, $\phi_2 = 0.03$) in 60:40 dioxan isopropanol

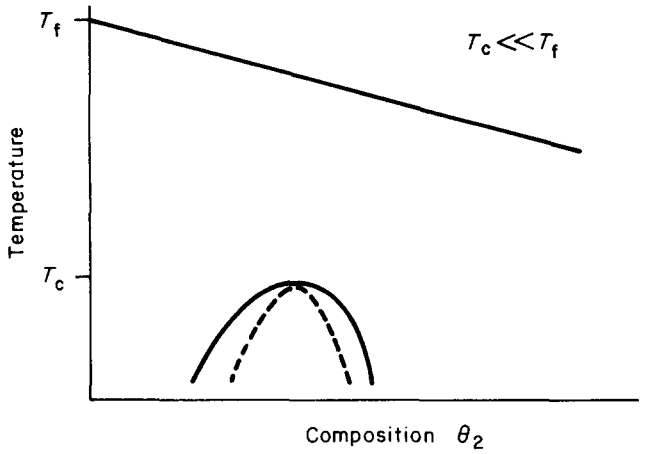

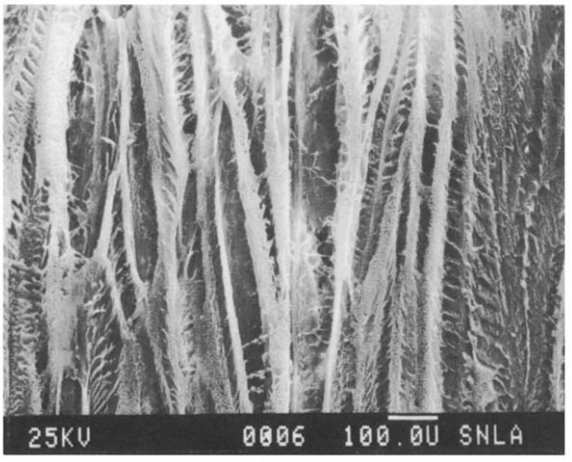

Figure 10 Pseudo two-component phase diagram and SEM of foam obtained for PS ($\bar{M}_n = 1.8 \times 10^6$, $\phi_2 = 0.03$) in 80:20 dioxan isopropyl alcohol

Table 1

$\bar{M}_n$	$[\eta]$ cm^3 g^{-1}	ϕ_2^*
5×10^4	18.34	0.052
2.33×10^5	39.58	0.024
6×10^5	63.52	0.015
1.8×10^6	110.0	0.009

thermal heat capacity, which have been cooled to $-100°C$ with liquid nitrogen. In general, lower temperatures allowed thicker samples to be made with finer structure. A lower limit on this temperature, however, was found below which thermal stresses crack the solid solvent (i.e., the frozen bar). For cyclohexane this temperature was about $-110°C$; and therefore, for this solvent a temperature of $-100°C$ was used on the cold plate. It is important that good heat transfer occur between the cold plate and the mould bottom. Hence, all surfaces were highly polished copper. Non-uniform cooling can create stresses in the frozen samples, which results in voids in the foam. Further to ensure uniform heat transfer, we used a heat transfer fluid on the cold plate. This was usually n-propyl alcohol, which did not freeze at $-100°C$. This gives molecular contact between the fluid and the two copper plates. Samples of thickness less than 1 cm freeze within 2 min. After freezing, the reduced pressure in the mould was released and the open mould was placed in a bottle connected to a vacuum pump for freeze-drying. Freeze-drying requires only that the sample remain totally frozen until all of the solvent sublimes. For solvents of relatively high melting point (e.g., CH, D, B), the endothermic evaporation of solvent was sufficient to keep samples frozen without any precautions (such as active cooling). For solvents of low melting point (e.g., alcohols as in D–I, B–I), it was necessary to insulate the freeze-drying bottle so that it did not warm up. With efficient insulation, it was still unnecessary to provide any active cooling. Foams which were made from solutions that were kept frozen and immobile during freeze-drying did not show any surface films. *Figure 11* shows SEM's of the top and bottom surface of an 'as-cast' polystyrene foam. No surface skin appears on either surface.

All of our foams show shrinkage during the freezing and the freeze-drying steps. In order to obtain the desired foam densities, it was necessary to 'dilute' the starting solutions relative to volume fractions corresponding to desired foam densities. The amount of shrinkage will depend upon the specifics of the process, such as the strength of vacuum in freeze-drying, and must be experimentally determined for each experimental setup. Our dilution factors are typically around 1.5.

Mould design

A representation of the mould currently used is shown in *Figure 12*. It consists of a copper bottom (1/8 in) and of

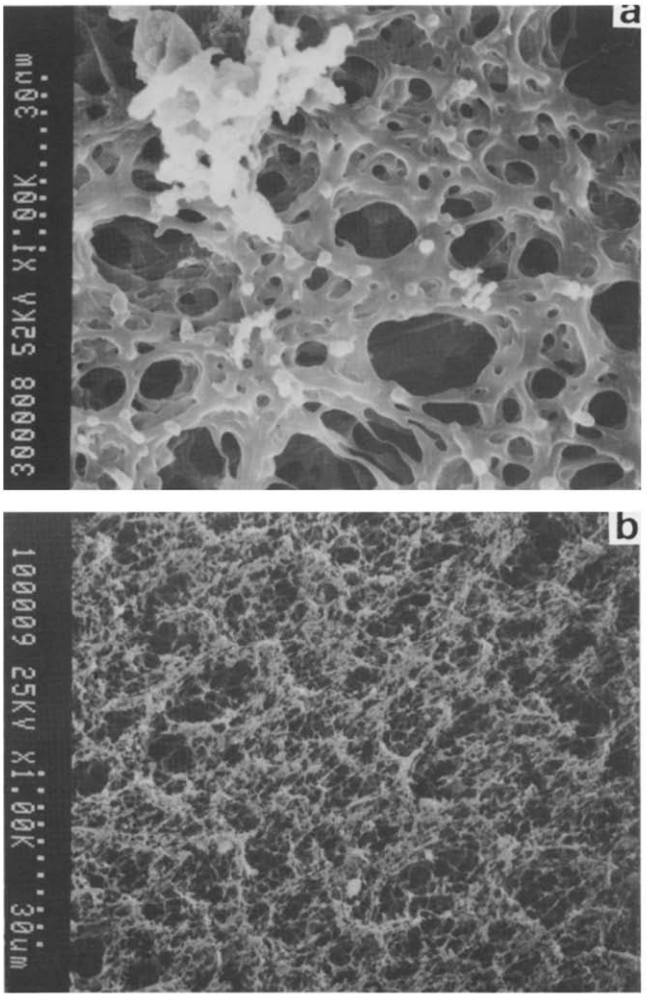

Figure 11 SEM's of the 'as molded' top (upper photo) and bottom (lower photo) of a PS foam of density, $\rho \simeq 0.05$ g cm^{-3}. No surface films are present with proper freeze-drying

epoxy sides and top. A valve is connected to the mould stide for degassing. The mould is filled upside down and inverted after degassing, at which time the bottom plate is held in place by vacuum. The important aspects of the mould are that it allows the solution within it to be degassed and that it ensures that the heat transfer is one-dimensional. One-dimensional heat transfer is necessary because the solution shrinks when it is frozen. If the heat transfer occurs in more than one dimension, then a void or crack occurs where the freezing fronts meet.

Additives

A variety of additives have been successfully incorporated into these foams at low concentrations. This has been accomplished by using additives (for example organic compounds such as dyes) that are soluble in the polymer solution. Assuming that the solubility of the additive in the polymer and solvent are of the same order of magnitude, when the solution phase-separates most of the additive remains in the polymer-poor phase since that phase typically accounts for about 90% or more of the solution volume (for a polymer volume fraction of 0.10). After freezing the solvent it is removed by freeze-drying. If the additives are non-volatile solids, they crystallize over the polymer structure as the solvent evaporates away. This results in an additive distribution which is uniform on a length scale greater than the cell size. We expect that by choosing the solubility properties of the additive, solvent and polymer, it should be possible to devise systems for which additives might be selectively incorporated either uniformly within the polymer phase, or else coated exclusively on the surface of the foam. The ability readily to prepare foams having a thin, uniform surface coating of an additive offers a number of interesting possibilities. Surface modification could allow control of important material properties of the foam – for instance hydrophilicity. The small cell size and high surface area of the foam materials could make them of interest as a substrate or support for additive coatings intended to serve as catalysts. Coated microcellular foams might also be of interest for chromatography or filtration applications.

CONCLUSIONS

We have developed a technique to produce low-density microcellular polystyrene foams with densities of 0.02–0.2 g cm^{-3} and cell sizes of 1–20 μm. The technique, although described for polystyrene, is applicable to any polymer for which appropriate solvents are available. By using well-characterized polymers, we have been able to relate foam morphology and cell size to solution thermodynamics and dynamics. The morphology is determined either by liquid–liquid or liquid–solid phase separation. The latter gives foams with an anisotropic, sheet-like morphology, while the former gives isotropic foams with small cell sizes.

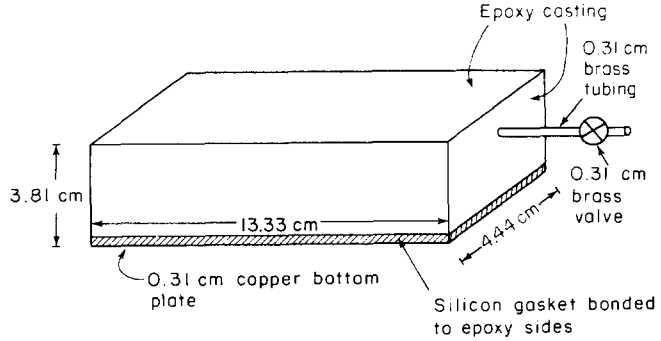

Figure 12 Sheet moulds currently in use

Some evidence was presented indicating that the liquid–liquid phase separation was spinodal. Good agreement was obtained between predictions of Cahn's theory for the structure of a spinodally decomposed binary liquid and the foam morphology and cell size if the early stage spinodal structure were captured. The important parameters for producing high-quality foams are:

(1) choice of solvent having a θ temperature for the polymer of interest which is above the freezing point,
(2) rigorous degassing prior to freezing, and
(3) rapid, unidirectional cooling of the solution. Cell size

Cell size can be controlled by varying solvent composition, quench rate, and polymer molecular weight. It is possible to incorporate additives by inclusion of soluble compounds in the solution before casting.

ACKNOWLEDGEMENTS

We wish to thank E. Russick and C. Quintana for producing the foams used in this study. C. Quintana designed the moulds currently in use. D. Doughty, W. Even and R. Carling provided input on mould design and processing. Valuable technical advice was given by A. Young, M. Shaw, P. Rand and J. Curro. M. Shaw suggested that the mechanism may involve spinodal decomposition.

REFERENCES

1 Aubert, J. H. Symposium on 'Applications of Phase Diagrams in Polymer Science', National Bureau of Standards, Gaithersburg, MD, USA, October 1984
2 Coudeville, A., Eyharts, P., Perrine, J. P., Rey, L. and Rouillard, R. *J. Vac. Sci. Technol.* 1981, **18**, 1227
3 Young, A. T., Moreno, D. K. and Marsters, R. G. *J. Vac. Sci. Technol.* 1982, **20**, 1094
4 Rand, P. B. 'Very Low Density Microcellular Foams', Fusion Target Fabrication Meeting; GA Technologies, Inc., San Diego, CA, April, 1984
5 Young, A. T. Symposium on 'Applications of Phase Diagrams in Polymer Science', National Bureau of Standards, Gaithersburg, MD, USA, October, 1984
6 Castro, A. J. U.S. Patent 4,247,498, November 24, 1978
7 Rinde, J. A. U.S. Patent 4,012,265, March 15, 1977
8 Smolders, C. A. *Polym. Sci. Technol.* 1980, **13**, 161
9 Flory, P. J. 'Principles of Polymer Chemistry', Cornell University Press, Ithaca, New York, USA, 1953
10 Brandrup, J. and Immergut, E. H. (Eds.), 'Polymer Handbook', 2nd Edn. 1975
11 Hodgman, C. D. (Ed.) 'Handbook of Chemistry and Physics', 44th Edn. 1961
12 Fujita, H. and Teramota, A. 'Polymer Compatibility and Incompatibility', Solc, K. (Ed.), Harwood Academic Publishers, Chur, Switzerland, 1982, pp. 125–138
13 Olabisi, O., Robeson, L. M. and Shaw, M. T. 'Polymer–Polymer Miscibility', Academic Press, New York, USA, 1979
14 Huston, E. L., Cahn, J. W. and Hilliard, J. E. *Acta Metal.* 1966, **14**, 1053
15 Cahn, J. W. *J. Chem. Phys.* 1965, **42**, 93
16 Debye, P. *J. Chem. Phys.* 1959, **31**, 680
17 Bird, R. B., Armstrong, R. C. and Hassager, O. 'Dynamics of Polymeric Liquids: Vol. I', John Wiley and Sons, New York, USA, 1977
18 de Gennes, P. G. 'Scaling Concepts in Polymer Physics', Cornell University Press, Ithaca, New York, USA, 1979